Journal of Applied Polymer Science

Influence of Copolymer Fraction Composition in Ultrahigh Molecular Weight Polyethylene Blends with Ethylene/1-Hexene Copolymers on Material Physical and Tensile Properties

T. M. Ushakova, E. E. Starchak, V. G. Krasheninnikov, V. G. Grinev, T. A. Ladygina, L. A. Novokshonova

Semenov Institute of Chemical Physics, Russian Academy of Sciences, Moscow 119991, Russia

Correspondence to: T. M. Ushakova (Email: tatiana567@mail.ru)

ABSTRACT: The reactor blends (RBs) with bimodal molecular weight distribution on the base of ultrahigh molecular weight polyethylene (UHMWPE) and low molecular weight random ethylene/1-hexene copolymers (CEH) were synthesized by two-step processes including ethylene polymerization followed by ethylene/1-hexene copolymerization over *rac*-$(CH_3)_2Si(Ind)_2ZrCl_2$/methylaluminoxane catalyst. The four series of blends differed in a composition of copolymer fraction that was varied in a wide range (from 3.0 to 37.0 mol % of 1-hexene). The differential scanning calorimetric study shows the double melting behavior of the net semicrystalline CEHs, which can be attributed to intramolecular heterogeneity in chain branch distribution. The introduction of CEHs leads to the modification of nascent RB crystalline and amorphous phases. Physical and tensile properties as well as melting indexes of the materials depend not only on the percentage of copolymer fraction that varied from 6.9 to 35.8 wt % but also on its composition. The increase of copolymer fraction with high content of 1-hexene ($\geq$11.0 mol %) in the blends leads to the change of the character of stress–strain curves; the materials behave as elastomers. Controlled regulation of copolymer fraction characteristics in the synthesis yields RBs combining the enough high strength, good plastic properties with enhanced melting indexes as compared with the net UHMWPE. © 2013 Wiley Periodicals, Inc. J. Appl. Polym. Sci. **2014**, *131*, 40151.

KEYWORDS: polyolefins; copolymers; blends; morphology; polyethylene; reactor blends; crystallinity; density; mechanical properties

Received 21 June 2013; accepted 2 November 2013

DOI: 10.1002/app.40151

INTRODUCTION

Polyethylene (PE) is one of the most claimed, large-scale polyolefin. The numerous types of PE produced in the world are classified by a structure, density, mechanical properties, melting indexes, and other characteristics to determine a product application and processing operations. An effective method of PE morphology, physical, and mechanical properties regulation is an introduction of short-chain branches into polymer chain. The copolymerization of ethylene and higher α-olefins such as 1-butene, 1-hexene, or 1-octene with metallorganic catalysts is a common way of linear low density PE (LLDPE) of controlling crystallinity and density preparation. Another way of the directional change of PE-based materials morphology and improvement of their mechanical and processing properties is a formation of polymer compositions, including the components that differ in the molecular weight as well as the content, length, and distribution of branches. The compositions of high density PE (HDPE) with LLDPE or HDPE with branched low density PE, characterized by the bimodal structural and molecular weight distributions, are obtained traditionally by the blending of components in the melt. The effect of component characteristics on the mechanical blend morphology, physical, and mechanical properties is discussed in the numerous papers.[1–6]

The methods for preparation of polyolefin compositions directly in the synthesis are developed now. The important feature of these methods is the possibility to obtain the reactor blends (RBs) including ultrahigh molecular weight polyolefins. An industrial method based on multireactor technological schemes consists in the processes of sequential olefin homo- and co-polymerization in the presence of metallorganic catalysts.[7–9] A two-step process of ethylene polymerization followed by copolymerization of ethylene with higher α-olefin with homogeneous[10,11] or immobilized[12] metallocene catalysts, carried out in a single reactor, is an analogue of this industrial method. A combination of two types of catalysts with different ability to introduce the higher α-olefin into polymer chain also applies for the preparation of RBs in one-step polymerization process.[13–15]

Contrary to the conventional Ziegler–Natta catalysts, metallocene systems allow one to control the polymer product microstructure and properties through the metallocene compound design and to obtain polyolefins with different molecular weight and copolymers with high α-olefin content, narrow molecular weight distribution and high compositional uniformity.[16–20] This makes it possible to vary the structure and properties of RB components in a wide range.

Earlier, we examined two-step processes of ethylene polymerization followed by copolymerization of ethylene with 1-hexene or 1-octene over homogeneous zirconocene catalysts Cp_2ZrCl_2/methylaluminoxane (MAO) and *rac*-$Et_2(Ind)_2ZrCl_2$/MAO.[10,11] It was shown that the copolymers with adjusted microstructure and molecular weight can be introduced into HDPE by this method. A number of RBs of HDPE with weight-average molecular weight (Mw) 320,000 g/mol and ethylene/1-hexene copolymer (CEH) of the same composition characterized by improved mechanical properties as compared with net HDPE have been obtained. The effect of molecular weight characteristics of the individual components and the content of copolymer fraction in RBs on the material properties were investigated by Shan et al.[12] when using two series of blends synthesized with immobilized zirconocene catalysts. These RBs were based on HDPE with low or high Mw and ethylene/1-octene copolymers of the same composition and of high and low Mw, respectively.

It would be interesting to obtain and investigate the RBs of ultrahigh molecular weight PE (UHMWPE) with CEH of different compositions and low Mw to find out the influence of the copolymer characteristics on the RB physical and mechanical properties and to develop the understanding of relationships between structure and properties of the material. It would be also very important to clarify the possibility to improve the processability of the UHMWPE.

In this study, the four series of RBs based on UHMWPE and CEHs of low molecular weight, different comonomer content and, respectively, the number of butyl brunches per 1000 carbon atoms were synthesized in two-step processes, including ethylene polymerization followed by ethylene/1-hexene copolymerization in the presence of *rac*-$(CH_3)_2Si(Ind)_2ZrCl_2$/MAO catalyst. A melting behavior, crystallinity, density, tensile properties, and melting indexes of RBs were investigated as a function of copolymer composition and its content in the material.

EXPERIMENTAL

Materials

The zirconium compound *rac*-dimethyl-silylenebis(1-η^5-indenyl) zirconium dichloride [*rac*-$Me_2Si(Ind)_2ZrCl_2$] and MAO as a 10% solution in toluene were used as received from Aldrich Co. Toluene (spectroscopic grade, Aldrich Co) was held over molecular sieves 5 Å and distilled from sodium wire in an argon atmosphere. Ethylene was polymerization grade. 1-Hexene was held over molecular sieves and was distilled from sodium wire in an argon atmosphere. The C_6H_{12} fraction, boiling at 64°C, was collected.

Polymerization

The one-step polymerization processes of ethylene polymerization as well as ethylene/1-hexene copolymerization were carried out at 30°C in toluene in 400 mL glass reactor while vigorously stirring and temperature-controlled. The reactor was pumped and was charged with 150 mL toluene, MAO solution, estimated amount of 1-hexene (in the case of ethylene/1-hexene copolymerization) and the zirconium compound. Then, it was heated to the 30°C, and ethylene was admitted into the system. Ethylene pressure and polymerization temperature during the run were maintained constant. In order to terminate the polymerization, a 5% HCl solution in ethanol was introduced into reactor. The resulting polymer product was filtered, washed with ethanol, and vacuum-dried at 60°C.

Two-step polymerization processes were carried out in the reactor described above. The reactor was pumped and charged with 150 mL toluene, MAO solution, and zirconium compound. Then, it was heated to 30°C, and ethylene was admitted into the system. After a certain time of ethylene polymerization, the estimated amount of 1-hexene was introduced into reactor, containing synthesized PE, to start the step of ethylene/1-hexene copolymerization. Both steps of the sequential process were carried out at the constant ethylene concentration. No more than 0.4 g of copolymer was synthesized in the copolymerization step to avoid a high 1-hexene conversion. As a result, the RB consisting of HDPE and copolymer with necessary content of polymer components was formed directly in the synthesis. The amounts of HDPE and copolymer fractions in the blend were calculated from the consumption of ethylene in polymerization step and copolymerization one. The content of comonomer in the polymer product was considered in the case of copolymerization step. In order to terminate the polymerization, a 5% HCl solution in ethanol was introduced into reactor. The resulting RB was filtered, washed with ethanol, and vacuum-dried at 60°C.

Polymer Analysis

The molecular-weight characteristics of the polymers (Mw, Mn, and Mw/Mn) were measured by the gel permeation chromatography (GPC) on a Waters 150C chromatograph in 1,2,4-trichlorobenzene at 140°C.

The contents of 1-hexene in the pure copolymers ([H], mol %) were determined by ^{13}C NMR spectroscopy.[21] The ^{13}C NMR spectra of 10–15% copolymer solutions in *ortho*-dichlorobenzene were recorded at 393 K on an AM 400 WB spectrometer operating at 100.6 MHz. A special high temperature, high-resolution sensor, which has a separate channel of the magnetic field stabilization with the tuned to the frequency of the 2H nucleus external RF coil with a tiny vial containing hexadeuterodimethylsulfoxide was used. The number of butyl branches per 1000 carbon atoms in the copolymers was calculated by a formula:

$$CH_3/1000C = 1000 \times [H]/(2\,(100-[H]) + 6 \times [H]). \quad (1)$$

Infrared analysis was also applied to calculate the composition of CEHs synthesized in the one-step copolymerization and in the copolymerization steps of sequential processes. IR spectra were recorded with Bruker FTIR Tensor 27 spectrophotometer. The branch contents ($\alpha = CH_3/1000C$) in the polymer samples were determined using the spectral band at 1378 cm^{-1}.[22] The

Table I. The Conditions of One-Step Ethylene/1-Hexene Copolymerization and Copolymerization Step of Two-Step Processes, the Properties of Obtained Net CEHs and Copolymer Fractions of RBs[a]

	Polymerization conditions				Copolymer characteristics		
			[H] (mol %)				
Run	$[C_6H_{12}] \times 10^2$ (mol/L)	f	^{13}C NMR	IR[b]	CH_3/1000C	Mw (g/mol)	MWD
One-step ethylene/1-hexene copolymerization							
1	2.4	0.45	3.0	3.2	14	249,500	2.5
2	5.3	1.0	6.3	-	28	-	-
3	8.0	1.5	8.0	-	34	155,564	2.3
4	11.6	2.2	10.9	11.1	45	131,100	2.3
5	20.0	3.8	19.0	17.9	67	110,000	2.5
6	54.0	10.2	37.0	35.7	106	63,000	2.5
Ethylene/1-hexene copolymerization after ethylene pre-polymerization							
7	2.4	0.45	-	2.8	14	-	-
8	11.6	2.2	-	11.0	45	-	-
9	20.0	3.8	-	18.5	67	-	-
10	54.0	10.2	-	36.5	106	-	-

[a] 30°C, $[C_2H_4] = 5.3 \times 10^2$, mol/L, [*rac*-$Me_2Si(Ind)_2ZrCl_2$] $= 5 \times 10^{-5}$ mol/L, molar ratio [Al] : [Zr] = 2500.
[b] The values [H] = [H^{RB}] for copolymer fractions are based on an average of all samples of each series of RBs.

contents of 1-hexene in the pure copolymers and in the copolymer fractions of RBs ([H]^{RB}, mol %) were calculated by the formulas (2) and (3), respectively:

$$[H] = \alpha \times 100/2(500-2\alpha) \quad (2)$$

$$[H]^{RB} = \alpha Q_E \times 100/2(500-2\alpha)Q_E^{II} \quad (3)$$

where $Q_E = Q_E^{I} + Q_E^{II}$—ethylene consumption in the homopolymerization step (Q_E^{I}, mol) and in the copolymerization step (Q_E^{II}, mol) of sequential process.

The product melting endotherms were obtained using Differential Scanning Calorimeter DSC 204 F1 Phoenix, NETZSCH-Gerätebau GmbH. The samples were heated to 160°C at the heating rate 10°C/min, cooled at 10°C/min to room temperature to erase the previous thermal history, and heated at 10°C/min for recording the melting events. The crystallinity of the samples (χ) was estimated by comparing DSC melting enthalpy at the second heating to that of a perfect PE crystal ($\Delta H = 289$ J/g). DSC melting endotherms at the first heating were used for the analysis of heating behavior of the nascent materials.

The density of polymer products was determined by the method of hydrostatic weighting, using *n*-heptane as working fluid.

Tensile properties were determined at the mode of sustained tension of samples using universal testing machine "JJ Instruments" at 25°C and the rate of sample deformation 1 min^{-1}. The samples in the form of double-sided blades were cut from the plates with the thickness of 0.5 mm. The plates were made by the method of hot pressing at 190°C and pressure 10 MPa. All the reported mechanical parameters are based on an average of a minimum of five samples. The sample melting indexes were estimated using IIRT-5 (Russia) at 190°C under the loads 2.16, 5.0, 10.6, and 21.6 kg (GOST 11645-73).

RESULTS AND DISCUSSION

Synthesis and Composition of Reactor Blends

The one-step processes of ethylene/1-hexene copolymerization as well as ethylene homopolymerization in the presence of *rac*-$(CH_3)_2Si(Ind)_2ZrCl_2$/MAO were investigated previously to choose the conditions of each polymerization step of the sequential processes including ethylene homopolymerization followed by ethylene/1-hexene copolymerization for the synthesis of RBs on the base of UHMWPE and CEHs of different composition. The one-step processes of ethylene homopolymerization were studied at 30°C and ethylene concentrations from 5.4×10^{-2} to 9.0×10^{-2} mol/L. It was shown that UHMWPE with Mw $\sim$ 1,000,000 g/mol and molecular weight distribution (MWD) = 3.3 is formed at $[C_2H_4] = 9.0 \times 10^{-2}$ mol/L. These conditions were used in the first step of the two-step processes for the synthesis of UHMWPE fraction of RBs. The conditions of investigated one-step ethylene/1-hexene copolymerization as well as the copolymerization step of two-step sequential processes, the properties of obtained net CEHs and CEH fractions of RBs are presented in Table I. The content of 1-hexene ([H], mol %) in the net copolymers were calculated using ^{13}C NMR and IR spectral dada; there was a good convergence of the results.

The content of 1-hexene in the copolymer fractions of RBs was calculated from IR spectral data as described in "Experimental" ([H^{RB}]). It is seen that in the presence of *rac*-$(CH_3)_2Si(Ind)_2ZrCl_2$/MAO, as well as Cp_2ZrCl_2/MAO and *rac*-$Et_2(Ind)_2ZrCl_2$/MAO[10,11] catalysts, ethylene pre-polymerization does not affect the copolymer composition. The content of 1-hexene in RB copolymer fraction depends on the conditions of copolymerization step and coincides with this one in the net copolymers, obtained under the same conditions.

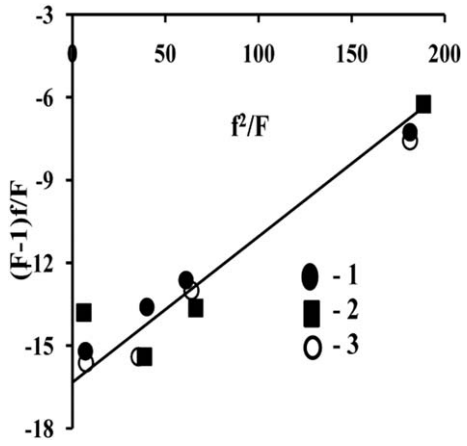

Figure 1. The dependence of *F* on f in the Fineman-Ross coordinates for the net CEHs and copolymer fractions of RBs. 1—*F*, calculated from ^{13}C NMR data, for the net CEHs; 2—*F*, calculated from IR data, for the net CEHs; 3—*F*, calculated from IR data, for CEH fractions of RBs.

Figure 1 demonstrates the Fineman-Ross plot of $F = [H]/[E]$ (where [E] is ethylene units content, mol %) or $F = [H^{RB}]/[E]$ versus rations of comonomer concentrations in the reaction zone $f = [C_6H_{12}]/[C_2H_4]$ for CEHs synthesized both in the one-step copolymerization and in the copolymerization step of the sequential processes, respectively. The relative reactivity constants of ethylene ($r_E = 16.2$) and 1-hexene ($r_H = 0.06$) were determined by using Figure 1 data. The value of $r_E \times r_H = 0.98$ is close to 1, indicating the formation of random CEHs in the presence of used catalyst.

Four series of RBs on the base of UHMWPE and CEHs with ~ 3.0, 11.0, 19.0, and 37.0 mol % of 1-hexene were synthesized. These copolymer fractions are, respectively, labeled in Table II as CEH-1, CEH-2, CEH-3, and CEH-4. Copolymer fraction percentage in the series of RBs was from 6.9 to 35.8 wt %. The compositions of RBs are presented as the ratio of the PE and copolymer fractions contents (UHMWPE/CEH) in wt %.

Figure 2(a) demonstrates the MWD curves for the net UHMWPE, net CEH-2 and RB on their base with 35.8 wt % of copolymer fraction. Peak in the low molecular part of MWD curve of RB represents its copolymer fraction. It is seen that positions of RB copolymer fraction and net CEH-2 peaks coincide. This means that ethylene pre-polymerization does not affect the molecular weight characteristics of copolymer part of RBs. Molecular weight characteristics of the copolymer fractions of RBs, presented in Table II, are based on the GPC data for the net CEHs.

The introduction of copolymers with low molecular weight into UHMWPE leads to the decrease of average Mw of polymer product (Table II). Such RBs including components with narrow MWD (3.3 for UHMWPE and 2.3–2.5 for copolymer fractions) are characterized by the broad MWD (5.0–7.9). The RBs UHMWPE/CEH-2 [Figure 2(a)], UHMWPE/CEH-3 and

Table II. Composition of RBs and Their Characteristics

				DSC data, second heating				MI at 190°C and the load (kg)			
RB series	UHMWPE/CEH (wt %/wt %)	Mw (g/mol)	MWD	t_1 (°C)	t_2 (°C)	χ (%)	Density (g/cm^3)	21.6	10.6	5.0	2.16
UHMWPE	100/0	1,000,000	3.3	140.0	0	54.3	0.971	0	0	0	0
UHMWPE/CEH-1	90/10	-	-	136.6	0	38.3	-	0	0	0	0
	79.7/20.3	-	-	135.4	102	35.4	-	0	0	0	0
	69.5/30.5	-	-	132.8	108	24.3	-	0	0	0	0
CEH-1	0/100	249,500	2.5	0	119.7/104.8	30.1	-	-	-	-	-
UHMWPE/CEH-2	100/0	1,000,000	3.3	140.0	0	54.3	0.971	0	0	0	0
	93.1/6.9	416,000	5.2	135.0	0	41.0	0.942	0.03	0	0	0
	83.3/16.7	414,000	5	134.7	0	35.5	0.937	0.3	0.01	0	0
	64.2/35.8	397,300	5.8	131.4	0	29.7	0.935	-	1.6	0.47	0.1
CEH-2	0/100	131,100	2.3		120.0/71.1	7.3	-	-	-	-	-
UHMWPE/CEH-3	100/0	1,000,000	3.3	140.0	0	54.3	0.971	0	0	0	0
	91/9	461,300	5.8	138.0	0	41.4	0.930	5.3	0	0	0
	82.5/17.5	-	-	137.0	0	31.8	0.922	8.6	0.6	0	0
	69.5/30.5	370,000	6.0	134	0	25.0	0.919	-	2.5	0.67	0.11
CEH-3	0/100	110,000	2.5	0	0	0	-	-	-	-	-
UHMWPE/CEH-4	100/0	1,000,000	3.3	140.0	0	54.3	0.971	0	0	0	0
	92.2/7.8	400,000	6.7	126.0	0	33.0	0.926	-	3.1	0.14	-
	68.5/31.5	350,000	7.9	108.3	0	22.5	0.902	-	-	9.2	3.0
CEH-4	0/100	63,000	2.5	0	0	0	-	-	-	-	-

-, No determined.

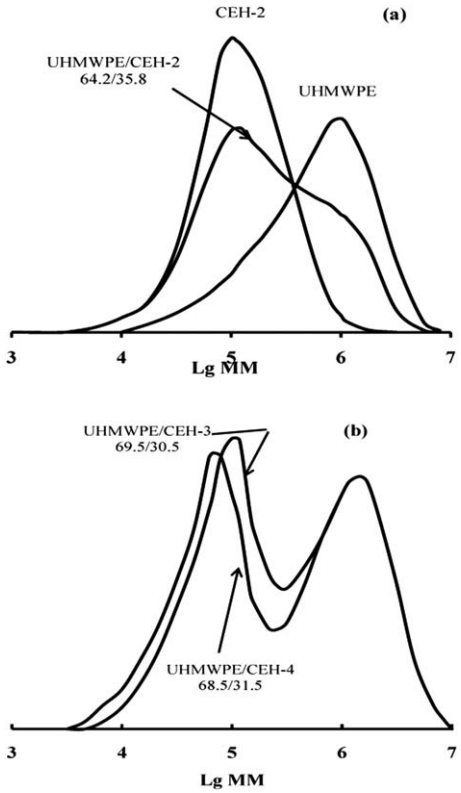

Figure 2. MWD-curves of the reactor blends.

UHMWPE/CEH-4 [Figure 2(b)] with copolymer fraction content ~30 wt % have clearly marked bimodal MWD.

Thus, the comparison of the compositions of CEHs obtained in the one-step copolymerizations and in the second copolymerization steps of sequential processes as well as GPC analysis of RBs show that the sequential two-step process including ethylene homopolymerization and ethylene/1-hexene copolymerization with *rac*-$(CH_3)_2Si(Ind)_2ZrCl_2$/MAO catalyst is the effective method for the introduction of random CEH fraction of desired composition and Mw into UHMWPE.

Morphology of UHMWPE, Ethylene/1-Hexene Copolymers, and Reactor Blends on Their Base

DSC melting endotherms for the net random CEHs of different composition and content of branches synthesized in one-step ethylene/1-hexene copolymerization (Table I, runs 1–4) are presented in Figure 3. All of them display two melting peaks. The first peak in the region of low temperatures shifts from 104.8 to 61.2°C as the amount of branches in CEH increases from 14/1000C to 45/1000C or from 3.0 to 11.0 mol % of 1-hexen, respectively. The second melting peak is in the region of ~120°C and its intensity decreases with increasing copolymer branch density. This peak is almost indistinguishable on the DSC curves for CEHs with 34/1000C and 45/1000C (8.0 and 11.0 mol % of 1-hexen, respectively). At last, no peaks are on the DSC traces of CEHs with 67/1000C and 106/1000C (19.0 or 37.0 mol % of 1-hexen; Table I, runs 5, 6), indicating that these copolymers are completely amorphous.

The profiles of CEH melting endotherms are very similar to those of random metallocene CEH with branch density 17.9/1000C[23] and copolymers of different compositions, described by Waymouth and coworkers.[24] In contrast to random CEHs studied, last CEHs were characterized by double melting behaviors and the presence of a small amount of crystallinity in copolymers, containing up to ~ 40 mol % of comonomer. According to Ref. 24, these copolymers, obtained in copolymerization over MAO-activated unbridged mixed-ligand zirconocene catalyst with $r_E \times r_H = 2$, contained much more long methylene sequences compared with random CEHs of the same compositions.

The double melting behaviors of metallocene CEHs may be explained by the presence of two lamellar populations of different thermal stability and different lamellar thickness.[23,24] However, ethylene/α-olefin copolymers prepared with metallocene catalysts, including *rac*-$(CH_3)_2Si(Ind)_2ZrCl_2$/MAO, have narrow interchain distribution of comonomers.[16,19,20,24] Puig et al.[25] have compared multiple melting behavior of the semicrystalline ethylene/1-octene copolymers of the similar composition prepared with metallocene and titanium-based Ziegler-Natta catalysts. These copolymers had, respectively, narrow and wide interchain distribution of 1-octen units. The authors have concluded that contrary to Ziegler-Natta copolymer, multiple melting behavior of metallocene one can be attributed to intramolecular heterogeneity in the chain branch distribution. Methylene sequences between branch points of different length present in the studied metallocene random CEHs. The long sequences give high temperature peak at ~120°C. Obviously, the disappearance of this peak with increasing branches in CEH can be explained by the decreasing number of such long sequences.

The DSC data for nascent RBs of UHMWPE with semicrystalline CEH-1 and CEH-2 are given in Figure 4(a,b), respectively. The data concerning the second heating of RBs are presented in Table II. For UHMWPE/CEH-1 of 79.7/20.3 and 69.5/30.5, the two distinct melting peaks are observed, whereas there is only one peak when CEH-1 content is 10.0 wt %, as shown in Figure 4(a) and Table II. The presence of two peaks indicates that separate crystallization of PE (high temperature peak t_1)

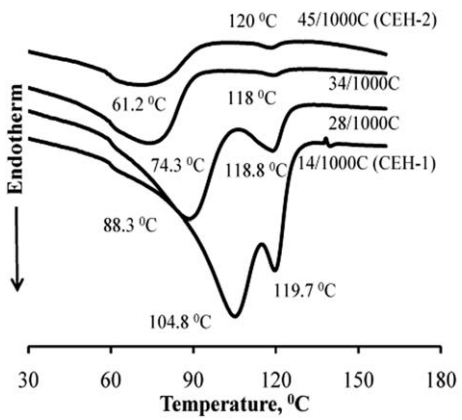

Figure 3. DSC melting endotherms for CEHs synthesized in one-step ethylene/1-hexene copolymerization (the second heating).

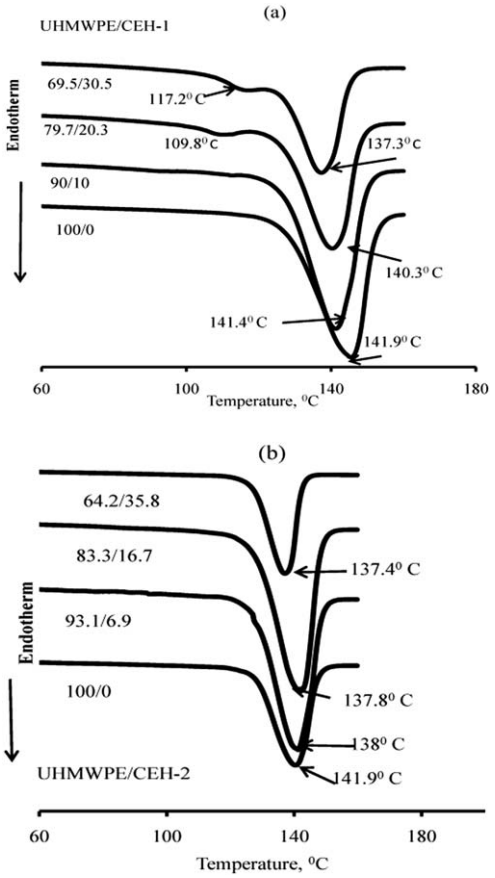

Figure 4. DSC heating curves of nascent UHMWPE/CEH-1 (a) and UHMWPE/CEH-2 (b).

and copolymer (low temperature peak t_2) fractions of RBs occurs in the blends with 20.3 and 30.5 wt % of CEH-1. However, the position of t_1 shifts to lower temperature with an increase of the CEH-1 content. It means that the peaks correspond to the PE crystalline phase containing a portion of CEH-1. That is, in these cases, separate crystallization takes place in the blends, but components are not completely separated and partial cocrystallization occurs between UHMWPE and CEH-1. There are the single endotherm peaks t_1 on DSC curves of all UHMWPE/CEH-2 blends [Figure 4(b), Table II]. This indicates that there is only one crystalline phase in these blends and two components form cocrystallites through all the range of CEH-2 percentage. The melting point of cocrystallites decreases with increasing the CEH-2 content. This means that the co-lamellae become thinner.

All blends with completely amorphous CEH-3 and CEH-4 show the single t_1 peaks on DSC curves both at the first and the second heating. The decrease of t_1 also takes place with the introduction of these copolymers into UHMWPE (Table II). For nascent UHMWPE/CEH-3 and UHMWPE/CEH-4 samples, t_1 changes from 141.9 to 131.7°C and from 141.9 to 135.4°C, respectively.

A phenomenon of cocrystallization between two components is well known for mechanical blends based on HDPE and semicrystalline LLDPE-s.[1,2,26–28] The DSC data obtained in our work for all series of RBs at the first heating testify that the presence of copolymer affects the crystallization processes occurring in the nascent reactor polymer blends. The cocrystallization of polymer components takes place directly in the preparation of RBs based on UHMWPE and semicrystalline CEH-1 and CEH-2. In the case of RBs, including completely amorphous copolymers CEH-3 and CEH-4, at least some of copolymer segments can be incorporated into growing PE crystal lattice, as Krishnaswamy et al.[5] suggested for mechanical blends of HDPE with amorphous copolymers. As a result, the less regular crystalline phase is formed. The decrease of melting temperature of PE part of material with the increase of copolymer fraction content observed for all investigated RBs is due to the formation of thinner lamellas as compared with the net UHMWPE.

The modification of UHMWPE by copolymers is accompanied by the decrease of material crystallinity (χ) and density (D) (Table II). Besides, the modification of RB amorphous phase takes place. Raman spectroscopic investigations of the prepared in this work nascent polymer products revealed that the increase of copolymer fraction content in the RBs leads to the decrease of trans-conformers in the material amorphous phase. In distinction from the net UHMWPE, the amorphous phase of RBs for the most part consists of gauche-conformers.[29,30]

Tensile Properties and Melting Indexes of RBs

The study of tensile properties of the net UHMWPE and RBs showed that the character of stress–strain curves depends both on the copolymer content in the material and copolymer composition. All samples UHMWPE/CEH-1 behave like the net semicrystalline UHMWPE. But as can be seen from Figure 5(a), which illustrates the initial deformation behavior of these samples, the broadening of the yielding zone with increasing copolymer fraction takes place. Such phenomenon was observed by Soares et al. for RBs based on HDPE and ethylene/1-octene copolymers.[12]

UHMWPE/CEH-2 and UHMWPE/CEH-3 blends behave somewhat differently. Figure 5(b) demonstrates the stress–strain curves for UHMWPE/CEH-2 samples. The introduction of copolymer in the amount of 6.9 wt % leads to the broadening of the yielding zone compared with the net UHMWPE. The yield maximum becomes indistinguishable on the curve for UHMWPE/CEH-2 with 16.7 wt % of copolymer. The curve of RB with 35.8 wt % of copolymer fraction takes the form typical for elastomers. The sample of UHMPE/CEH-3 (69.5/30.5) and all samples of UHMWPE/CEH-4 (92.2/7.8, 68.5/31.5) also behave as elastomers.

The increase of copolymer fractions in RBs based on CEH-1 and CEH-2 is accompanied by the reduction of the material tensile modulus (E) and tensile stress at yield (σ_y). The values of E for UHMWPE/CEH-1 and UHMWPE/CEH-2 blends (Figure 6, curves 1, 2) as well as σ_y for UHMWPE/CEH-1 (curve 3) decrease almost linearly with the reduction of the material crystallinity. In the case of UHMWPE/CEH-2 blends, such dependence σ_y versus χ is not observed (Figure 6, curve 4). The values of σ_y for blends with $\chi = 41$ and 35.5% (content of CEH-2 in the blends 6.9 and 16.7 wt %, respectively) are

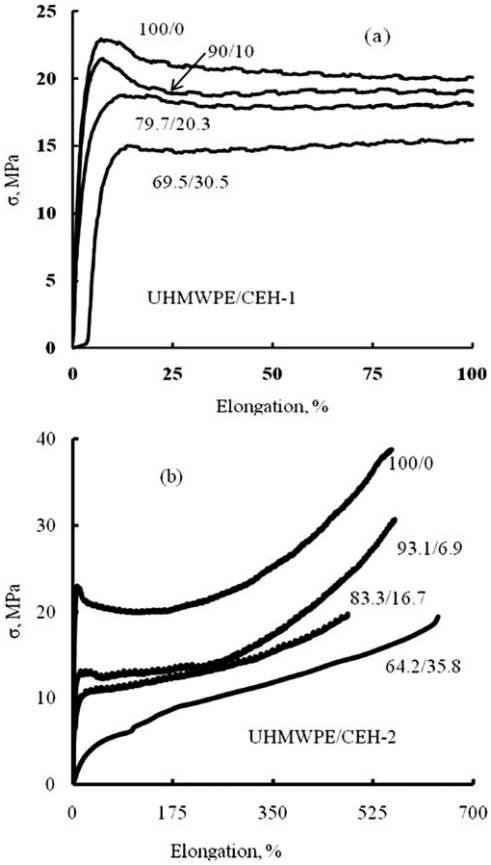

Figure 5. Initial parts of the stress–strain curves for UHMWPE/CEH-1 (a) and stress–strain curves for UHMWPE/CEH-2 (b).

close. Then, as was mentioned above, the tensile of UHMWPE/CEH-2 sample containing 35.8 wt % of copolymer ($\chi = 29.7\%$) occurs similar the elastomer materials. The yield stress is absent on the stress–strain curve of this material [Figure 5(b)].

Figures 7 and 8 represent the data concerning the change of tensile stress at break (σ_b) and elongation at break (ε_b) with increasing amount of the copolymer fraction in the blends with semicrystalline CEH-1 and CEH-2. For UHMWPE/CEH-1, except the sample 90/10, the σ_b magnitudes are close to that for

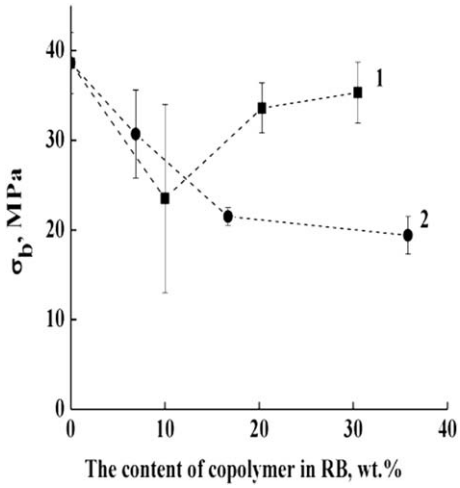

Figure 7. The curves σ_b versus content of copolymer in the reactor blends UHMWPE/CEH-1 (1) and UHMWPE/CEH-2 (2).

the net UHMWPE (Figure 7, curve 1). Elongations at break of these UHMWPE/CEH-1 samples are virtually independent of the copolymer content in RB (Figure 8, curve 1). Presumably, the large errors in the measurement of σ_b and ε_b of sample 90/10 are related to the material nonuniformity. The introduction of CEH-2 into UHMWPE leads to the decrease of material σ_b; nevertheless, these blends have the sufficiently high strength (Figure 7, curve 2). The value of elongation at break for UHMWPE/CEH-2 with 35.8 wt % of CEH-2 equals 640% and is slightly higher than that for the net UHMWPE (550%). Earlier, we found that the elongation at break of RB based on HDPE with Mw = 320,000 g/mol and CEH containing 4.0 mol % of comonomer with 30.0 wt % of copolymer fraction was 890% and 1.4-fold higher than that of the net HDPE.[9,10]

The RBs UHMWPE/CEH-3 and UHMWPE/CEH-4 with completely amorphous copolymers are characterized by low values of σ_b and ε_b.

The introduction of CEHs into UHMWPE by the reactor method may increase material melting index (MI). This characteristic depends on the copolymer composition and its content

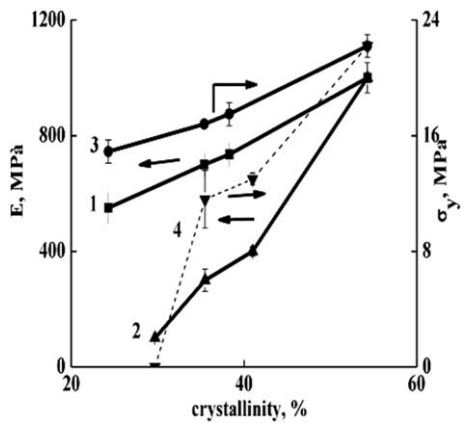

Figure 6. The dependence of E (1,2) and σ_y (3,4) on crystallinity of RBs UHMWPE/CEH-1 (1,3) and UHMWPE/CEH-2 (2,4).

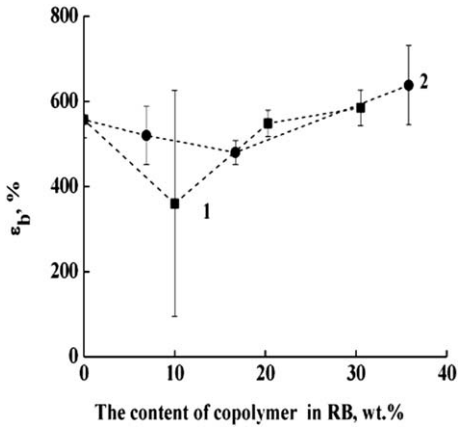

Figure 8. The curves ε_b versus content of copolymer in the reactor blends UHMWPE/CEH-1 (1) and UHMWPE/CEH-2 (2).

in RB. As it is seen from Table II, UHMWPE and its blends with CEH-1 do not flow at 190°C under the load 21.6 kg. At the same time, some RBs with CEH-2, CEH-3, and CEH-4 begin to flow under the load 10.6 kg. These RBs with ~30.0 wt % of copolymer fraction flow already under the loads 5.0 and 2.16 kg.

CONCLUSIONS

The two-step processes including the ethylene polymerization followed by ethylene/1-hexene copolymerization are the effective method for the preparation of the reactor PE blends with copolymer fraction of desired composition and properties. These two-step processes are the analogs of industrial processes based on the multireactor technological schemes and have no alternatives for the synthesis of UHMWPE blends. The introduction of CEHs leads to the modification of nascent RB crystalline and amorphous phases. The possibility to vary widely the composition and morphology of copolymer fraction from semicrystalline to completely amorphous in the polymerization with zirconocene catalyst allows one to affect the material crystallinity and density. Tensile properties and melting indexes of RBs depend not only on the properties of PE fraction and content of CEH fraction but are highly dependent on copolymer composition. Because of the presence of high number of interlamellar tie-molecules in PE fraction, UHMWPE blends with semicrystalline CEHs exhibit enough high strength. The introduction of CEHs with high content of comonomer provides blends with enhanced MI as compared with the net UHMWPE. Controlled regulation of copolymer fraction characteristics in the synthesis is a way for the preparation of materials based on UHMWPE that exhibit good tensile properties and improved processability.

REFERENCES

1. Puig, C. C. *Polym. Bull.* **1997**, *38*, 715.
2. Zhao, Y.; Liu, S.; Yang, D. *Macromol. Chem. Phys.* **1997**, *198*, 1427.
3. Godehardt, R.; Rudolph, S.; Lebek, W.; Goerlitz, S.; Adhikari, R.; Allert, E.; Geisemann, J.; Michler, G. H. *J. Macromol. Sci. Phys.* **1999**, *38*, 817.
4. Hussein, I. A.; Hameed, T. *J. Appl. Polym. Sci.* **2005**, *97*, 2488.
5. Krishnaswamy, R. K.; Yang, Q.; Fernandez-Ballester, L.; Kornfield, J. A. *Macromolecules* **2008**, *41*, 1693.
6. Kessner, U.; Kaschta, J.; Stadler, F. J.; Le Duff, C. S.; Drooghaag, X.; Munstedt, H. *Macromolecules* **2010**, *43*, 7341.
7. Gally, P.; Haylock, J. C.; Albizzati, E.; DeNicola, A. *Macromol. Symp.* **1995**, *98*, 1309.
8. Gally, P.; Collina, G.; Sgazzi, P.; Baruzzi, G.; Marchetti, E. *J. Appl. Polym. Sci.* **1997**, *66*, 1831.
9. Choi, Y.; Soares, J. B. P. *Can. J. Chem. Eng.* **2012**, *90*, 646.
10. Ushakova, T. M.; Meshkova, I. N.; Ladygina, T. A.; Grynev, V. G.; Novokshonova, L. A. *Polimery* **2001**, XLVI, 252.
11. Ushakova, T. M.; Meshkova, I. N.; Ladygina, T. A.; Grynev, V. G.; Novokshonova, L. A. *Polym. Sci. Ser. A* **2002**, *44*, 99.
12. Shan, C. L.; Soares, J. B. P.; Penlidis, A. *Polymer* **2002**, *43*, 7345.
13. Bruaseth, I.; Rytter, E. *Macromolecules* **2003**, *36*, 3026.
14. De Wet-Roos, D.; Dixon, J. T. *Macromolecules* **2004**, *37*, 9314.
15. Chien, J. C. W.; Iawamoto, Y.; Rausch, M.; Wedler, W.; Winter, H. *Macromolecules* **1997**, *30*, 3447.
16. Kaminsky, W. *Macromolecules* **2012**, *45*, 3289.
17. Resconi, L.; Cavallo, L.; Fait, A.; Piemontesi, F. *Chem. Rev.* **2000**, *100*, 1253.
18. Hung, J.; Cole, A. P.; Maymouth, R. M. *Macromolecules* **2003**, *36*, 2454.
19. Matsko, M. A.; Echevskaya, L. G.; Vanina, M. P.; Nikolaeva, M. I.; Mikenas, T. B.; Zakharov V. A. *J. Appl. Polym. Sci.* **2012**, *126*, 2017.
20. Mirabella, F. M.; Crist, B. *J. Polym. Sci. Part B: Polym. Phys.* **2004**, *42*, 3416.
21. Cheng, H. N. *Polym. Bull.* **1991**, *26*, 325.
22. Gol'denberg, A. L. *Jurnal Prikladnoi Spectroscopii* **1973**, *19*, 510.
23. Qiu, J.; Xu, D.; Zhao, J.; Niu, Y.; Wang, Z. *J. Polym. Sci. Part B: Polym. Phys.* **2008**, *46*, 2100.
24. Hung, J.; Cole, A. P.; Waymouth, R. M. *Macromolecules* **2003**, *36*, 2454.
25. Puig, C. C.; Aviles, M. V.; Joskowich, P.; Dias, A. *J. Appl. Polym. Sci.* **2001**, *79*, 2022.
26. Tashiro, K.; Stein, R. S.; Hsu, S. *Macromolecules* **1992**, *25*, 1801.
27. Tashiro, K.; Izuchi, M.; Kobayashi, M.; Stein, R. S. *Macromolecules* **1994**, *27*, 1228.
28. Tashiro, K.; Izuchi, M.; Kaneuchi, F.; Jin, C.; Kobayashi, M.; Stein, R. S. *Macromolecules* **1994**, *27*, 1240.
29. Zavgorodnev, Yu. V.; Prokhorov, K. A.; Novokshonova, L. A.; Ushakova, T. M.; Starchak, E. E.; Krasheninnikov, V. G.; Nikolaeva, G. Yu.; Sagitova, E. A.; Pashinin, P. P.; Guseva, M. A.; Donfack, P.; Von der Kammer, B.; Materny, *A. Laser Phys.* **2012**, *22*, 730.
30. Zavgorodnev, Yu. V.; Prokhorov, K. A.; Nikolaeva, G. Yu.; Sagitova, E. A.; Pashinin, P. P.; Ushakova, T. M.; Novokshonova, L. A.; Starchak, E. E.; Krasheninnikov, V. G. *Laser Phys.*, DOI: 10.1088/S1054660X13025701.